ELSEVIER

Ultrasonics 36 (1998) 25–29

Ultrasonics

Miniature drumheads: microfabricated ultrasonic transducers

I. Ladabaum [a,*], X.C. Jin, B.T. Khuri-Yakub

[a] E.L. Ginzton Laboratory, Stanford University, Stanford, CA 94305, USA

Abstract

Significant improvement in the performance of capacitive microfabricated ultrasonic transducers is reported and the modifications which enable the progress are described. Air-coupled through-transmission of glass and steel at 2.3 MHz is demonstrated for the first time. Furthermore, a 20 μm step on a silicon wafer is detected with both amplitude and phase signals at 3 MHz. The same process used to fabricate the air transducers also yields immersion transducers, which are reported to operate in water from 1 to 20 MHz with a dynamic range of 60 dB measured at 3 MHz. It is anticipated that optimized immersion transducers will be able to achieve the 110 dB dynamic range of the air transducers. A brief review of the theoretical modeling of the device is also presented. © 1998 Elsevier Science B.V.

Keywords: Air-coupled through-transmission; Capacitive ultrasonic transducer; Immersion transducer; Microfabrication process; Surface micromachining

1. Introduction

The serious study of ultrasound did not begin until after Pierre Curie's discovery of piezoelectricity in 1880 [1] and piezoelectric ceramics are still the basis of most ultrasonic transduction systems. Relatively recent interest in airborne ultrasonics, however, has motivated the development of capacitive transducers. Air-coupled ultrasound is useful in nondestructive evaluation (NDE) of materials and structures, in position detection systems and in gas flow metering applications, among other things. Although capacitively excited ultrasound has been investigated for decades [2–4], work with significant practical potential has coincided with the recent proliferation of microfabrication. The application of techniques pioneered by the IC industry to the fabrication of capacitive ultrasonic transducers has been reported in Refs. [5–7]. Perhaps the most advanced device and fabrication process was introduced in Refs. [8,9]. Further improvements found in Refs. [10–14] extended the performance and understanding of microfabricated ultrasonic transducers (MUTs) and have spurred on concurrent development efforts [15].

The current state of MUT development is that transducers have been shown to transmit and receive ultrasound in both air and water. MUTs are superior to piezoelectric transducers in air because their impedance more closely matches that of air. The use of air-coupled capacitive transducers to excite and detect resonant longitudinal modes in aluminum is described in Ref. [16] and the first demonstration of simple air-coupled through-transmission of aluminum is contained in Ref. [14]. In immersion applications, the mature piezoelectric technology still outperforms MUTS. However, it is anticipated that optimized MUTs will have performance competitive with that of piezoelectrics, with further advantages in temperature range, fabrication and electronic interrogation [11,12,14].

In this paper, we review the fabrication and modeling of MUTS. We then present the results of the latest experiments with the transducers, which prove that MUTs are applicable in air-coupled NDE and in profilometry. We present water transmission results and conclude with a brief discussion about device optimization and future work.

2. Device description

An MUT consists of metalized membranes (top electrode) suspended above heavily doped silicon bulk (bottom electrode). A schematic of one element of the

* Corresponding author. Tel: + 1-650-723-0150; Fax: + 1-650-725-7509; e-mail: igal@stanford.edu

PII S0041-624X(97)00134-0

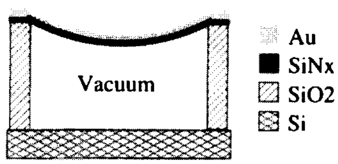

Fig. 1. Schematic of one element of an MUT.

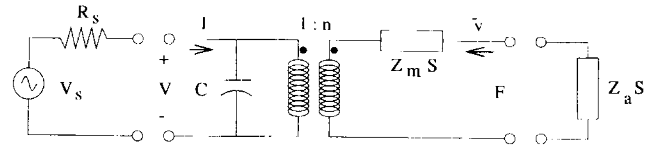

Fig. 3. Equivalent circuit which models the behavior of an MUT.

device is shown in Fig. 1. A transducer consists of many such elements, as shown in Fig. 2. When a DC voltage is applied between the two electrodes, Coulomb forces attract them together, while stress within the membrane resists the attraction. If the membrane is driven by an AC voltage, significant ultrasound generation results. Conversely, significant detection currents are generated when the membrane is biased appropriately and subjected to ultrasonic waves.

Each MUT element can be described by an electrical equivalent circuit model such as the one shown in Fig. 3. An entire device is the parallel combination of such elements. The model allows for the analysis and optimization of MUTS. In the model, the transformer ratio is:

$$n=\frac{V_{\mathrm{DC}}\epsilon_0\epsilon^2 S}{(\epsilon_0 l_\mathrm{t}+\epsilon l_\mathrm{a})^2}, \tag{1}$$

where V_{DC} is the bias voltage, S is the membrane area, ϵ_0 is the permitivity of vacuum, ϵ is the dielectric constant of the membrane material, l_t is the thickness of the membrane layer and l_a is the separation.

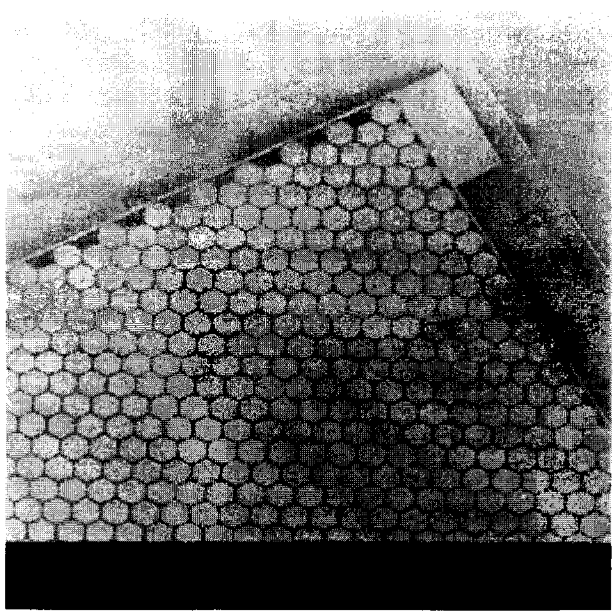

Fig. 2. SEM of a corner of a MUT with bond pad visible.

The mechanical impedance is:

$$\begin{aligned}Z_m=\frac{P}{\bar{v}}=&j\omega p l_\mathrm{t}\\&\times[j\omega p l_\mathrm{t} a k_1 k_2 (k_2 J_0(k_1 a) J_1(k_2 a)\\&+j\omega p l_\mathrm{t} k_1 J_1(k_1 a) J_0(k_2 a))]\\&/[a k_1 k_2 (k_2 J_0(k_1 a) J_1(k_2 a)+k_1 J_1(k_1 a) J_0(k_2 a))\\&-2(k_1^2+k_2^2) J_1(k_1 a) J_1(k_2 a)],\end{aligned} \tag{2}$$

where P is the external uniform pressure applied to the membrane, $\bar{v}$ is average velocity and a is the membrane radius. The derivation of the model is found in [14]. Fig. 4 shows good agreement between the electrical impedance predicted by the model and the impedance observed experimentally.

The transformer ratio n can be made larger by increasing the applied voltage or by decreasing the membrane and air gap thickness. Furthermore, the mechanical impedance is a strong function membrane thickness and radius. It is thus clear that transducer performance depends upon the geometric configuration of the device. As shown in Fig. 5, the transducer's air loaded resonant frequency shifts by about 3.5% from its 2.29 MHz nominal value when the cell radius changes 2% from its nominal value of 50 μm. Although such geometric dependence is desirable because it allows for the design of optimized transducers, it also implies that it is critically important to have a robust fabrication process,

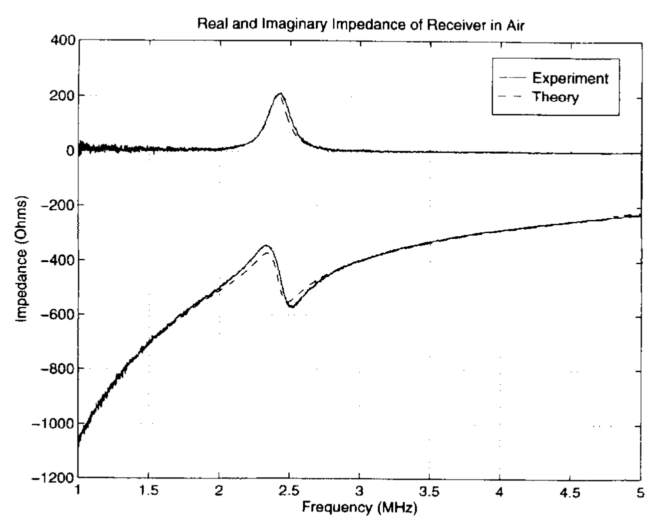

Fig. 4. Comparison of theoretical and experimental electrical impedance.

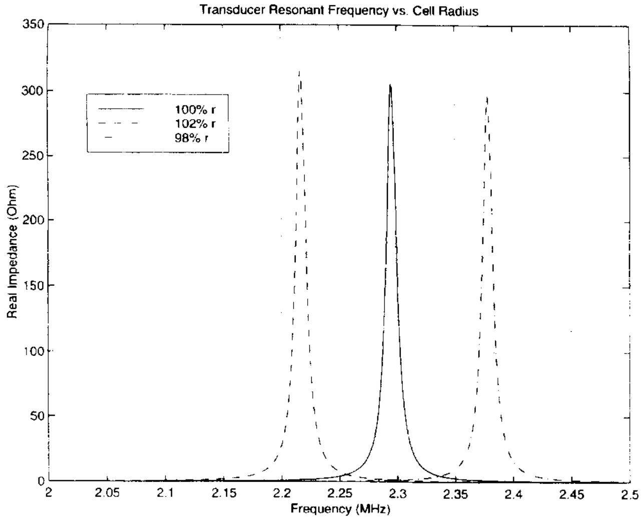

Fig. 5. Transducer resonant frequency change versus membrane radius.

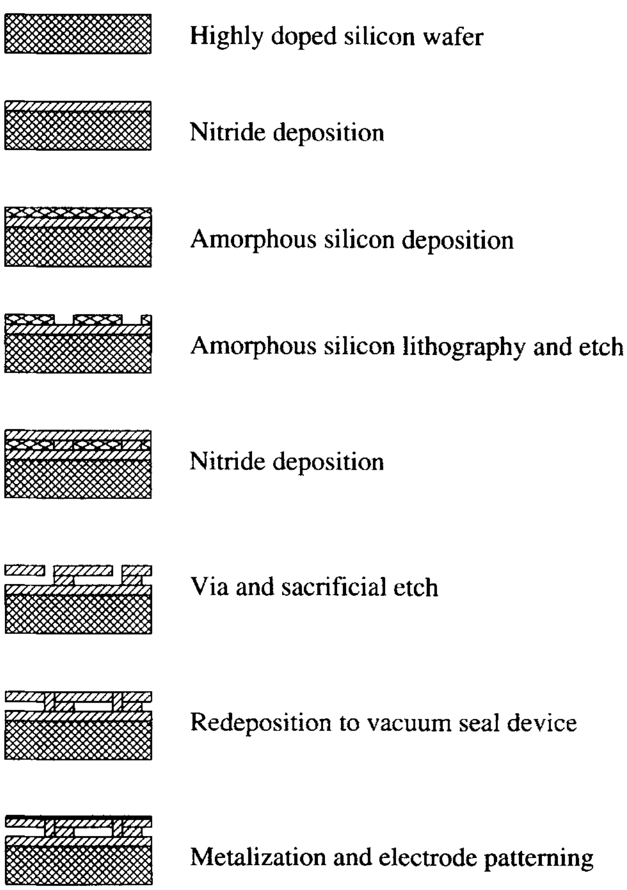

Fig. 6. Major steps of MUT fabrication.

especially for airborne transducers which operate in resonant mode and are made from a plurality of membranes. A fabrication process allowing for lithographic and chemical vapor deposition control of critical device dimensions is described in the following section and a more detailed treatment of fabrication issues is found in Ref. [13].

3. MUT fabrication

The fabrication scheme of the MUTs used to generate the results herein reported is found in Fig. 6. It is important to note that the device is completely surface micromachined, which implies that the high-volume fabrication of such transducers could be realized at a very low cost per transducer element. A 10 cm n-type (100) silicon wafer is heavily doped to achieve good conductivity at the wafer surface. A thin layer of LPCVD nitride is then deposited as an etch stop for the subsequent KOH sacrificial etch. Amorphous silicon is then deposited to form the sacrificial layer. Deposited amorphous silicon is patterned into hexagonally shaped islands to define the active transducer regions. A second layer of nitride is then deposited to form both the vibrating membrane and the cavity sidewalls. Both the residual stress of the film and membrane thickness affect the resonant frequency of the device. Vias are dry-etched to allow for the sacrificial etching in KOH, which removes the amorphous silicon, generating the acoustically active drumheads. For immersion devices, the via holes are closed by vacuum sealing with nitride or LTO deposition. The dimension of the via has implications on the mechanism with which the sealing is performed [13]. Finally, aluminum is sputtered and wet etch patterned to act as the top electrode. The same aluminum deposition also defines bonding contacts to the bottom electrode through a lithographically defined trench in silicon bulk. An SEM of the top view of the transducer is shown in Fig. 2.

4. Results

The results herein reported were obtained with the simple experimental set-up sketched in Fig. 7. The AC excitation signal is introduced with a 50 Ω function generator. The DC bias is provided by a regulated and filtered power supply. A custom transimpedance ampli-

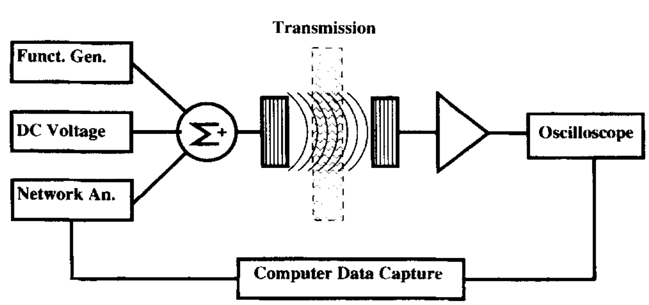

Fig. 7. Schematic of experimental set-up.

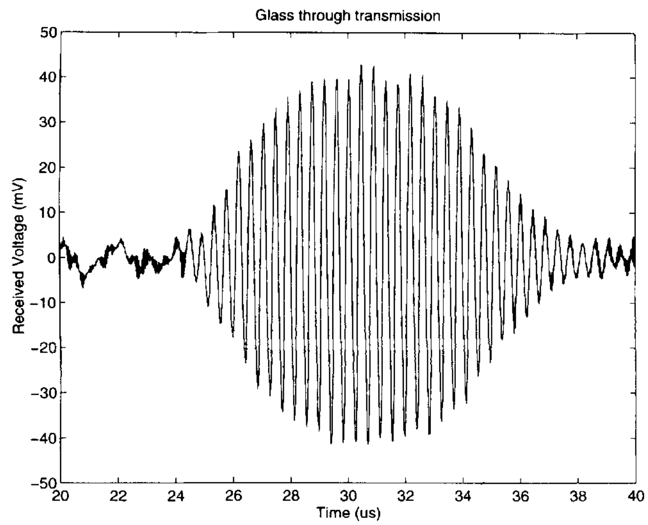

Fig. 8. Air-coupled through-transmission of glass.

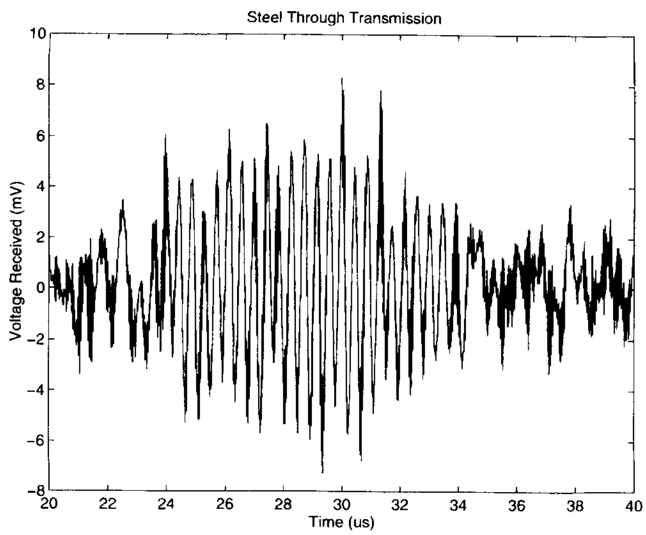

Fig. 9. Air-coupled through-transmission of steel.

fier conditions the received signal. Time domain data are captured with an 8 bit digitized oscilloscope. Frequency domain data are captured with a network analyzer protected from the bias voltages with a custom bias-T. Once captured, the data are transferred to a computer for display. In certain circumstances, data sample averaging is performed.

A dynamic range of 110 dB for an MUT transmission system operating in burst mode at 2.3 MHz is reported in [14]. Fig. 8 represents the first demonstration of the simple air-coupled through-transmission of ultrasound in glass. The transducers were placed approximately 1 cm apart and the glass slide had a thickness of 0.95 mm. A 20 cycle tone burst of 16 V was applied to the emitter and a 30 V bias was applied to both transmitter and receiver. The arrival time of the sound energy at 27 μs verifies a 9 mm separation of the transducers.

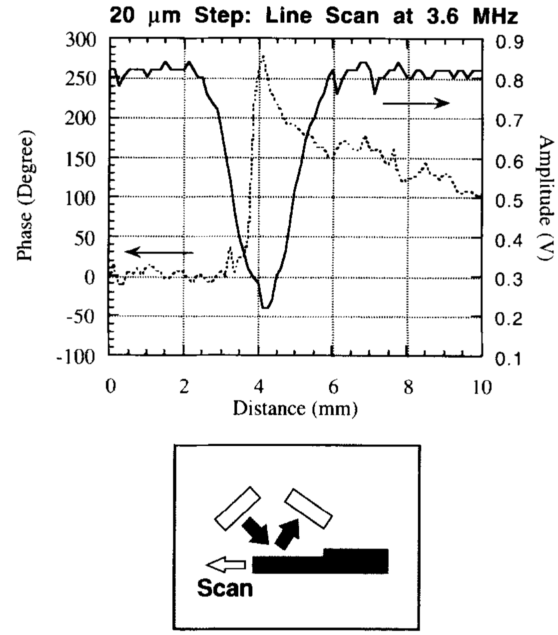

Fig. 10. Air transducer detection of a 20 μm step.

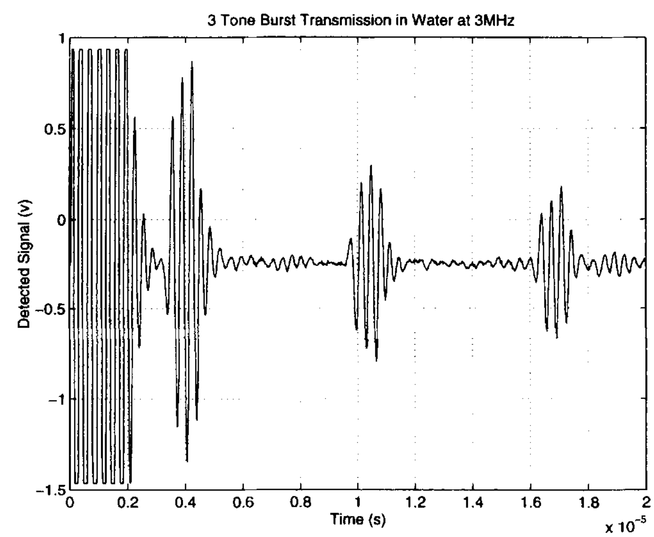

Fig. 11. Transmission and reception of ultrasound in water using MUTS.

Note that the SNR of the received signal is approximately 28 dB, which, when added to the 78 dB of expected loss from two glass–air interfaces and about 4 dB attenuation from 8 mm of air, confirms a dynamic range of 110 dB. A loss of approximately 90 dB is expected from two steel–air interfaces, which indicates that air-coupled through-transmission in steel should be possible. Such transmission was observed and is shown in Fig. 9, where the glass slide was replaced by a 1.7 mm steel shim. The SNR of the received signal appears to be below 20 dB and it could be due to suboptimal alignment or improper acoustic characterization of the steel sample. The significance of the air-coupled through transmission results is that they prove the eventual feasibility of air-coupled NDE.

Further proof of the utility of air transducers in practical applications is the step detection experiment depicted in Fig. 10. Two 3 MHz transducers were scanned over a 20 μm step on a silicon wafer in pulse-echo mode and the step was clearly detected in both phase and amplitude. Note that the amplitude represents the convolution of the 1 cm apertures of the transducers.

It has been claimed that the process can produce not only air transducers, but vacuum-sealed immersion devices. An unoptimized immersion transducer (that is, a transducer designed for air, but sealed in order to substantiate the process claim) was used to generate Fig. 11. When the receiver impedance is tuned with a serial inductor, a better than 60 dB SNR is observed in water transmission at 3 MHz. In future designs of immersion transducers, the geometry of the device (gap thickness, membrane thickness and radius) and bias voltage of the device can be modified to optimize the transducers for water operation, or more specifically, to increase the absolute value of the real part of the transducer impedance to the level comparable with the electronics.

5. Conclusion

This paper presents experimental results that prove the feasibility of MUTs in air-coupled NDE and profilometry. Water transmission results highlight the versatility of the microfabrication process. A fully surface micromachined fabrication scheme which will allow for the optimization of transducer designs based on theoretical understanding of transducer dynamics has been presented. It should also be appreciated that MUTs can operate at much higher temperature than piezoelectrics (they do not have a Curie temperature), that arrays can be fabricated at lower cost and that the electrical impedance of an MUT element can be designed to optimize the noise performance of receiver electronics. Future work will involve the realization of optimized transducers with improved fabrication processes and the use of the transducers in air and water coupled applications.

Acknowledgement

This work has been made possible by grants from the United States Office of Naval Research and fellowship support from the National University of Singapore. Special thanks are due to Dr Levent Degertekin for help with the step detection experiment and to Tom Carver, Pauline Prather and the staff of Stanford's nanofabrication facility.

References

[1] R.B. Lindsay, The story of acoustics, J. Acoust. Soc. Am. 39 (4) (1966) 629.

[2] W. Khul, G.R. Schodder, F.K. Schodder, Condenser transmitters and microphones with solid dielectric for airborne ultrasonics, Acoustica 4 (1954) 520–532.

[3] K. Matzuwa, Capacitive ultrasonic transducer, J. Phys. Soc. Jap. 13 (1958) 1533.

[4] J.H. Cantrell, J.S. Heyman, Broadband electrostatic acoustic transducer for ultrasonic measurements in liquids, Rev. Sci. Instrum. 50 (1) (1979) 31.

[5] K. Suzuki, K. Higuchi, H. Tanigawa, A silicon electrostatic ultrasonic transducer, IEEE Trans. Ultrason. Ferro. Freq. Control 36 (6) (1989) 620.

[6] M. Rafiq, C. Wykes, The performance of capacitive ultrasonic transducers using V-grooved backplates, Meas. Sci. Technol. 2 (2) (1991) 168.

[7] D.W. Schindel, D.A. Hutchins, L. Zou, M. Sayer, The design and characterization of micromachined air-coupled capacitance transducers, IEEE Trans. Ultrason. Ferroelec. Freq. Control 42 (1) (1995) 42.

[8] M.I. Haller, B.T. Khuri-Yakub, a surface micromachined electrostatic ultrasonic air transducer, in: Ultrasonics Symposium, Cannes, France, IEEE Ultrasonics, Ferroelectrics and Frequency Control Society, 1994, p. 1241.

[9] M.I. Haller, Micromachined ultrasonic devices and materials, Ph.D. thesis, Stanford University, 1997.

[10] I. Ladabaum, B.T. Khuri-Yakub, D. Spoliansky, M.I. Haller, Micromachined ultrasonic transducers MUTS, in: M. Levy, S.C. Schneider, B.R. McAvoy (Eds.), Ultrasonics Symposium, Seattle, Washington, IEEE Ultrasonics, Ferroelectrics and Frequency Control Society, 1995, p. 501.

[11] I. Ladabaum, B.T. Khuri-Yakub, D. Spoliansky, Micromachined ultrasonic transducers: 11.4 MHz transmission in air and more, Appl. Phys. Lett. 68 (1) (1996) 7.

[12] H.S. Soh, I. Ladabaum, A. Atalar, C.F. Quate, B.T. Khuri-Yakub, Silicon micromachined ultrasonic immersion transducers, Appl. Phys. Lett. 69 (24) (1996) 3674.

[13] X. Jin, I. Ladabaum, B.T. Khuri-Yakub, The microfabrication of capacitive ultrasonic transducers, in: Transducers 97, Chicago, IEEE Electron Devices Society, 1997, p. 437.

[14] I. Ladabaum, X.C. Jin, H.T. Soh, A. Atalar, B.T. Khuri-Yakub, Surface micromachined capacitive ultrasonic transducers, IEEE Trans. Ultrason. Ferro. Freq. Control, to appear.

[15] P. Eccardt, K. Niederer, T. Scheiter, C. Hierold, Surface micromachined ultrasound transducers in CMOS technology, in: M. Levy, S.C. Schneider, B.R. McAvoy, (Eds.), Ultrasonics Symposium, San Antonio, USA, IEEE Ultrasonics, Ferroelectrics, and Frequency Control Society, 1996, p. 959.

[16] D.W. Schindel, Air-coupled generation and detection of ultrasonic bulk-waves in metals using micromachined capacitance transducers, Ultrasonics 35 (2) (1997) 179.